

# Impact of Increasing Stratospheric Water Vapor on Ozone Depletion and Temperature Change

TIAN Wenshou<sup>\*1,2</sup> (田文寿), Martyn P. CHIPPERFIELD<sup>2</sup>, and LÜ Daren<sup>3</sup> (吕达仁)

<sup>1</sup>College of Atmospheric Science, Lanzhou University, Lanzhou 730000

<sup>2</sup>Institute for Climate and Atmospheric Science, School of Earth and Environment, University of Leeds, UK

<sup>3</sup>Institute of Atmospheric Physics, Chinese Academy of Science, Beijing 100029

(Received 28 May 2008; revised 3 October 2008)

## ABSTRACT

Using a detailed, fully coupled chemistry climate model (CCM), the effect of increasing stratospheric H<sub>2</sub>O on ozone and temperature is investigated. Different CCM time-slice runs have been performed to investigate the chemical and radiative impacts of an assumed 2 ppmv increase in H<sub>2</sub>O. The chemical effects of this H<sub>2</sub>O increase lead to an overall decrease of the total column ozone (TCO) by ~1% in the tropics and by a maximum of 12% at southern high latitudes. At northern high latitudes, the TCO is increased by only up to 5% due to stronger transport in the Arctic. A 2-ppmv H<sub>2</sub>O increase in the model's radiation scheme causes a cooling of the tropical stratosphere of no more than 2 K, but a cooling of more than 4 K at high latitudes. Consequently, the TCO is increased by about 2%–6%. Increasing stratospheric H<sub>2</sub>O, therefore, cools the stratosphere both directly and indirectly, except in the polar regions where the temperature responds differently due to feedbacks between ozone and H<sub>2</sub>O changes. The combined chemical and radiative effects of increasing H<sub>2</sub>O may give rise to more cooling in the tropics and middle latitudes but less cooling in the polar stratosphere. The combined effects of H<sub>2</sub>O increases on ozone tend to offset each other, except in the Arctic stratosphere where both the radiative and chemical impacts give rise to increased ozone. The chemical and radiative effects of increasing H<sub>2</sub>O cause dynamical responses in the stratosphere with an evident hemispheric asymmetry. In terms of ozone recovery, increasing the stratospheric H<sub>2</sub>O is likely to accelerate the recovery in the northern high latitudes and delay it in the southern high latitudes. The modeled ozone recovery is more significant between 2000–2050 than between 2050–2100, driven mainly by the larger relative change in chlorine in the earlier period.

**Key words:** stratospheric water vapor, temperature change, ozone depletion, chemistry-climate model

**Citation:** Tian, W. S., M. P. Chipperfield, and D. R. Lü, 2009: Impact of increasing stratospheric water vapor on ozone depletion and temperature change. *Adv. Atmos. Sci.*, **26**(3), 423–437, doi: 10.1007/s00376-009-0423-3.

## 1. Introduction

While the impact of CO<sub>2</sub> on the climate and ozone evolution has been studied extensively in the past (e.g., Pitari et al., 1992; Austin et al., 1992; Shindell et al., 1998; Rosenfield et al., 2002), the importance of stratospheric water vapor to ozone recovery and climate change has only recently been recognized. Observations of atmospheric water vapor concentrations have revealed significant increases during the last few decades (e.g., Nedoluha et al., 1998; Oltmans et al., 2000), while CCM simulations show that a sim-

ilar trend is likely to take place in the future atmosphere (e.g., Tian and Chipperfield, 2006). If this trend continues, it could affect stratospheric ozone recovery (Shindell, 2001). Increasing water vapor can give rise to not only a radiative cooling of the stratosphere (e.g., Rind and Logergan, 1995; Forster and Shine, 1999) but also affect chemical processes (e.g., Evans et al., 1998; Kirk-Davidoff et al., 1999). H<sub>2</sub>O-induced ozone changes can, in turn, cause radiative responses in the stratosphere. Water vapor is the source of HO<sub>x</sub> (=OH+HO<sub>2</sub>) radicals, which directly destroy O<sub>3</sub> in both the lower and upper stratosphere. The

---

\*Corresponding author: TIAN Wenshou, wstian@lzu.edu.cn

$\text{HO}_x$  species also interact with other chemical families, which in turn affect  $\text{O}_3$  loss.  $\text{H}_2\text{O}$  is also involved in heterogeneous chemistry in the lower stratosphere. Stratospheric water vapor can modify the formation of liquid and solid aerosol particles while heterogeneous chemical reaction rates depend on the aqueous content of liquid aerosols.

Stuber et al. (2001) have shown a crucial role of the stratospheric water vapor feedback for the forcing-response relationship in their GCM simulations. Forster and Shine (2002) pointed out that increases in stratospheric water vapor are capable of causing a radiative forcing of up to  $0.29 \text{ W m}^{-2}$  and a cooling of more than 0.8 K in the lower stratosphere over the past 20 years. Shine et al. (2003) analysed stratospheric temperatures from a range of different models and found that stratospheric water vapor changes have a significant impact on computed temperature trends. They pointed out that upper stratosphere water vapor can cause a  $0.2 \text{ K (10 yr)}^{-1}$  cooling and modelled temperature trends in the lower stratosphere can be significantly improved if the cooling effects of the increased water vapor are included. Using a 2-D radiative-chemical-dynamical model, Evans et al. (1998) investigated the chemical effects of the stratospheric water vapor and found that increasing stratospheric water vapor results in an enhancement of mid stratospheric ozone by 1%–2% and an increase of ozone depletion in the upper stratosphere. However, large differences exist in GCM results of radiative and chemical effects of increasing water vapor in the stratosphere (Oinas et al., 2001; Stenke and Grewe, 2005). Therefore, further investigation of chemical and radiative effects of increasing stratospheric water vapor are not only necessary but also important for making more reliable predictions of the future ozone layer and climate change (e.g., Dameris et al., 2001; Shindell and Grewe, 2002).

Smith et al. (2001) found, from the Halogen Occultation Experiment (HALOE) data, that water vapor trends between 1992–1999 range from  $80 \text{ ppbv yr}^{-1}$  in the upper stratosphere to  $20 \text{ ppbv yr}^{-1}$  at 50 hPa. Based on the longer record of stratospheric water vapor sampled at Boulder, a  $35\text{-ppbv yr}^{-1}$  trend throughout the stratosphere has been used in previous modelling studies (Dvortsov and Solomon, 2001). If the trends continue at the lower end of this range, it is possible that stratospheric water vapor could increase by around 2 ppmv by the end of this century. In this paper, we use a 3-D fully coupled chemistry-climate model (CCM) to diagnose chemical and radiative effects of a prescribed 2 ppmv stratospheric  $\text{H}_2\text{O}$  increase. We attempt to quantify the radiative and chemical effects of the stratospheric water vapor sep-

arately with this interactively coupled CCM. We also present a prediction of the ozone layer by 2100. The details of the model and numerical experiments are described in section 2. The chemical effects of increasing water vapor are addressed in section 3. In section 4, the radiative effects of increasing stratospheric water vapor are discussed. An integrated perspective of the potential influences of stratospheric water vapor on the ozone layer and temperature, as well as tracer transport, is given in section 5. The effect of stratospheric water vapor on ozone recovery is discussed in section 6, and our conclusions are summarized in section 7.

## 2. Model setup and integrations

The CCM used in this study has a latitude-longitude resolution of  $2.5^\circ \times 3.75^\circ$  and 64 levels extending from the surface to 0.01 hPa (approximately 80 km). The model is based on the Met Office Unified Model (UM) v4.5 (Cullen, 1993) with a detailed, interactively coupled, stratospheric chemistry scheme from the established SLIMCAT chemical transport model (Chipperfield, 1999). The coupled model advects 28 chemical tracers with around 42 chemical species including the  $\text{O}_x$ ,  $\text{HO}_x$ ,  $\text{Cl}_y$ ,  $\text{Br}_y$ , and  $\text{NO}_y$  families and source gases. The model includes both gas-phase chemistry and heterogeneous chemistry on liquid and solid aerosols and polar stratospheric clouds (PSCs). The model's chemical  $\text{O}_3$ ,  $\text{N}_2\text{O}$ , and  $\text{CH}_4$  tracers are coupled to the UM's radiation scheme. The chemistry is calculated on 30 levels spanning 150 hPa to 0.5 hPa. A more detailed description of the CCM can be found in Tian and Chipperfield (2004). Six CCM integrations have been performed for this study and their basic configurations are given in Table 1. The values of GHGs used in the model simulations are listed in Table 2 and the sea-surface temperatures and sea-ice fields are the same in all the experiments. The control run R0 uses 2000 GHG values from the IPCC scenario A2 (World Meteorological Organization, 2003) as listed in Table 2 and  $\text{O}_3$ ,  $\text{N}_2\text{O}$ , and  $\text{CH}_4$  concentrations from the chemistry module are coupled to the UM's radiation scheme. In run R0, the water vapor field from the chemistry module is not used in the UM's radiation scheme; the UM humidity field is used instead. Run R1 is the same as R0 except that the water vapor from the chemistry scheme is increased by 2 ppmv everywhere from 150 hPa to 0.5 hPa. Run R2 is the same as R0 except chemistry water vapor is used in the UM's radiation scheme. In run R3, the water vapor calculated by the chemistry scheme is increased by 2 ppmv and passed to the model's radiation scheme. Runs R4 and R5 are the same as R2 except that 2050 and 2100 GHG values from the IPCC A2 scenario are

**Table 1.** Six 10-year time-slice model experiments.

Run	Year of GHG Values	+2 ppmv H <sub>2</sub> O	Radiation coupling
R0	2000		O <sub>3</sub> , N <sub>2</sub> O, CH <sub>4</sub>
R1	2000	In chem. scheme	O <sub>3</sub> , N <sub>2</sub> O, CH <sub>4</sub>
R2	2000		O <sub>3</sub> , N <sub>2</sub> O, CH <sub>4</sub> , H <sub>2</sub> O
R3	2000	In rad. scheme	O <sub>3</sub> , N <sub>2</sub> O, CH <sub>4</sub> , H <sub>2</sub> O
R4	2050		O <sub>3</sub> , N <sub>2</sub> O, CH <sub>4</sub> , H <sub>2</sub> O
R5	2100		O <sub>3</sub> , N <sub>2</sub> O, CH <sub>4</sub> , H <sub>2</sub> O

**Table 2.** The values of greenhouse gases (GHGs) used in the model simulations.

Year	CO <sub>2</sub> (ppmv)	N <sub>2</sub> O (ppbv)	CH <sub>4</sub> (ppbv)	CFC11 (pptv)	CFC12 (pptv)
2000	368	316	1760	262	540
2050	532	373	2562	105	350
2100	856	447	3731	34	212

used, respectively. Note that in all the runs, the stratospheric O<sub>3</sub>, N<sub>2</sub>O, and CH<sub>4</sub> values for the radiation scheme are taken from the chemistry module. From R0 and R1 we attempt to diagnose chemistry related effects of increasing H<sub>2</sub>O on ozone depletion. From R2 and R3 we investigate the chemical and dynamical responses to the stratospheric cooling induced by increasing H<sub>2</sub>O. From R2, R4, and R5 we try to understand the ozone layer by 2100. All model diagnostics are 10-year averaged climatologies, unless stated otherwise. Note that the stratospheric water vapor is predicted by the chemistry module and has no interaction with the tropospheric water vapor in the CCM (constant boundary conditions for all the chemical species are given at 150 hPa to represent the tropospheric input).

Those idealised time slice runs are usually better when extended to more than 10 years to avoid the potential effect of interannual variability on model climatologies. However, Tian and Chipperfield (2004) found that the modelled variability of the CCM used in this study is not as significant as expected due to the fixed SSTs for each year. Further 20-year test runs indicate that the results from the 10-year time slice runs are overall consistent with those from the longer experiments.

### 3. Chemical effects of increasing water vapor

Here we assess the chemical impacts of a 2-ppmv stratospheric water vapor increase on the temperature and ozone depletion from experiment R0 and R1. Figure 1 shows the total column ozone (TCO) differences between R0 and R1. Also shown are the vortex-averaged ozone and temperature differences. An increase of 2-ppmv water vapor in the chemistry scheme leads to a decrease in the TCO at southern high lati-

tudes and an increase at northern high latitudes. An overall decrease of the TCO (about 1%) in the tropics is evident. The largest changes in the TCO occur in the polar regions with a maximum decrease of 20 DU in the Antarctic and a maximum increase of 17 DU in the Arctic. In terms of the percentage of TCO changes, a maximum decrease of about 12% is caused in the Antarctic in November and a maximum increase of around 6% in the Arctic in January. The temperature responses to the chemical increase of H<sub>2</sub>O are mainly caused by changes in the solar heating as a result of the O<sub>3</sub> changes. In the southern high latitude winter, a 2-ppmv H<sub>2</sub>O increase results in a 1–2 K warming in the stratosphere. Evident warming of the stratosphere can also be noted at the northern high latitudes, with a maximum of 2 K in January. In the tropical stratosphere, the temperature is decreased by 0.5 K accompanying the 1% TCO decrease.

The vortex-averaged differences show that ozone concentrations in the run with a 2-ppmv increase of stratospheric water vapor in the chemistry scheme (R1), are about 0.1 ppmv higher than those in the control run R0 in the middle and upper Arctic stratosphere. The Arctic vortex temperature in R1 is about 1–2 K cooler than in R0 from December to January, and about 1 K warmer from February to March. In the middle and upper Antarctic stratosphere, the vortex-averaged ozone concentrations in R1 are larger than in R0 from June to July, but up to 0.2-ppmv lower from August to October. The Antarctic winter vortex temperature in R1 is about 1–2 K warmer than in R0 and the magnitude of this warming of the polar stratosphere increases with height. We can see that temperature changes between R0 and R1 are not simply related to the ozone changes in the vertical and time distribution. However, the vortex-averaged differences are overall in accordance with the column ozone dif-

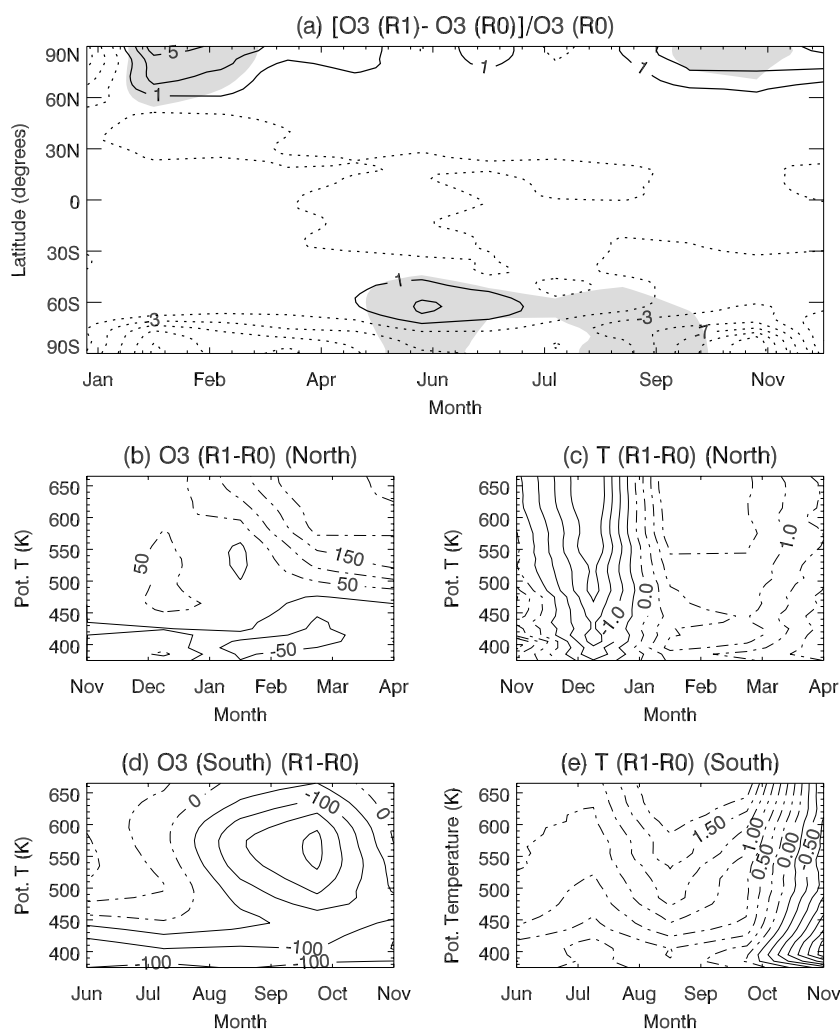


**Fig. 1.** (a) Differences (%) in the TCO between R0 and R1. The contour interval is 2% for ozone changes. The regions where the stratospheric temperature in R1 (averaged between 100–10 hPa) is more than 1 K warmer than in R0 are shaded. (b)–(e) Vortex-averaged temperature (K) and ozone differences (ppbv) between R0 and R1 for the NH and SH winter/spring. The solid (dashed) lines represent negative (positive) contours. The vortex boundary was taken as the  $65^\circ$  equivalent potential vorticity latitude contour.

ferences at high latitudes between R0 and R1.

Figure 2 shows latitude-height cross sections of the percentage of change of ozone concentrations and temperature differences between R0 and R1. Also shown are the differences in chemical ozone loss,  $\text{NO}_x$ ,  $\text{Cl}_x$  and  $\text{Br}_x$  concentrations. The chemical ozone loss is defined as  $\text{O}_3 - \text{O}_{3p}$ , where  $\text{O}_{3p}$  is a passive ozone tracer, which is reset in the model every June and December. In the upper stratosphere, ozone concentrations decrease by 1%–6% due to the extra 2 ppmv  $\text{H}_2\text{O}$ , while in the middle stratosphere, the ozone mixing ratios increase by 1%–5%. Correspondingly, the temperature in the upper stratosphere in R1 is 1–2 K cooler than in R0, while the temperature in the middle stratosphere

of the high latitudes in R1 is 1–2 K warmer. Evans et al. (1998) also showed that increasing water vapor increases ozone concentrations in the mid stratosphere by 1%–2% and enhances ozone destruction in the upper stratosphere. In the middle and upper stratosphere, the chemical loss term dominates the transport term in the ozone tendency equation. In consequence, differences in the chemical ozone loss are most pronounced here. In general, chlorine and  $\text{NO}_x$  cycles dominate the mid-upper stratospheric ozone depletion. The corresponding height-latitude cross sections of the zonal mean  $\text{Cl}_x$  and  $\text{NO}_x$  fields indicate that  $\text{Cl}_x$  concentrations in R1 are overall larger than those in R0, while ozone changes between R0 and R1 are in accor-

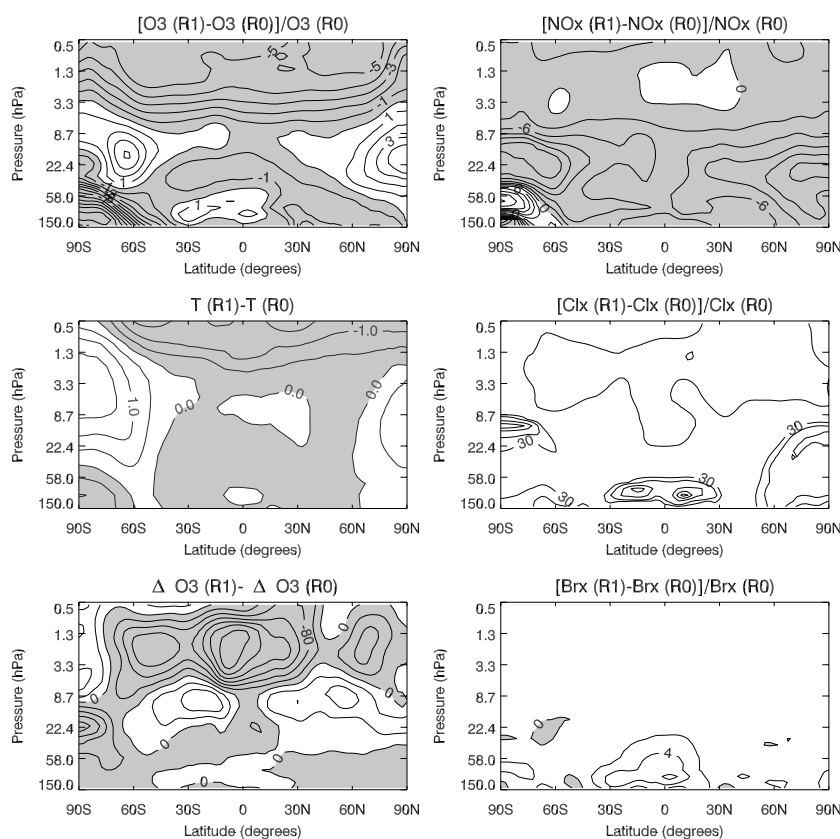


**Fig. 2.** Latitude-height cross sections of the percentage of change in the annual mean ozone between R0 and R1. The corresponding changes in the temperature, chemical ozone loss,  $\text{NO}_x$ ,  $\text{Cl}_x$ , and  $\text{Br}_x$  are also shown. The contour interval is 1 K for temperature differences and 40 ppbv for chemical ozone loss. The contours for the other fields are in %. The regions with negative contours are shaded.

dance with corresponding  $\text{NO}_x$  changes with an anti-correlation between them in the middle stratosphere. In the tropics, ozone concentrations are increased by 1%–2% in the lower stratosphere due to 2 ppmv extra  $\text{H}_2\text{O}$ , and decreased by 1%–2% in the mid stratosphere. In principle, the tropical lower stratospheric ozone loss is dominated by the  $\text{HO}_x$  catalytic cycle. Increasing  $\text{H}_2\text{O}$  gives rise to more  $\text{HO}_x$  and hence more  $\text{O}_3$  loss. Meanwhile, an increase in OH tends to remove  $\text{NO}_2$  by the increased production of  $\text{HNO}_3$ , and hence to depress  $\text{O}_3$  depletion in the middle stratosphere at higher latitudes. Figure 2 suggests that ozone changes in the tropical lower stratosphere are not only controlled by  $\text{HO}_x$  but also related to  $\text{Cl}_x$  and  $\text{Br}_x$ , as the  $\text{Cl}_x$  and  $\text{Br}_x$  changes are rather large in the tropical lower stratosphere.

From Fig. 1 we have seen that the net chemical effect of increased  $\text{H}_2\text{O}$  is to decrease the tropical column ozone. The maximum decrease of ozone (about 12%) due to a 2-ppmv  $\text{H}_2\text{O}$  increase occurs in the southern high latitudes lower stratosphere. The chemical

ozone destruction in the winter and spring at high latitudes is primarily caused by gas-phase catalytic cycles that involve ClO radicals. Due to the warming of the middle and upper stratosphere at the southern high latitudes, the ClO-related destruction of ozone tends to be suppressed in R1. However, in the southern high latitudes lower stratosphere, there seems to be larger ozone destruction in R1, accompanied by relatively large  $\text{NO}_x$  changes. Figure 3 gives the  $\text{NO}_x$  and  $\text{Cl}_x$  ( $=\text{Cl}+\text{ClO}+2\text{Cl}_2\text{O}_2$ ) fields from R0 and R1. The run with increased  $\text{H}_2\text{O}$  (R1) shows larger values of active chlorine ( $\text{Cl}_x$ ) in the polar spring regions. This is due to the enhanced PSC activity in R1 with increased  $\text{H}_2\text{O}$  and is the cause of the larger chemical ozone losses.

#### 4. Radiative effects of increasing water vapor

When the water vapor in the model's radiation scheme is increased by 2 ppmv, the direct response is a cooling of the stratosphere by no more than 2 K

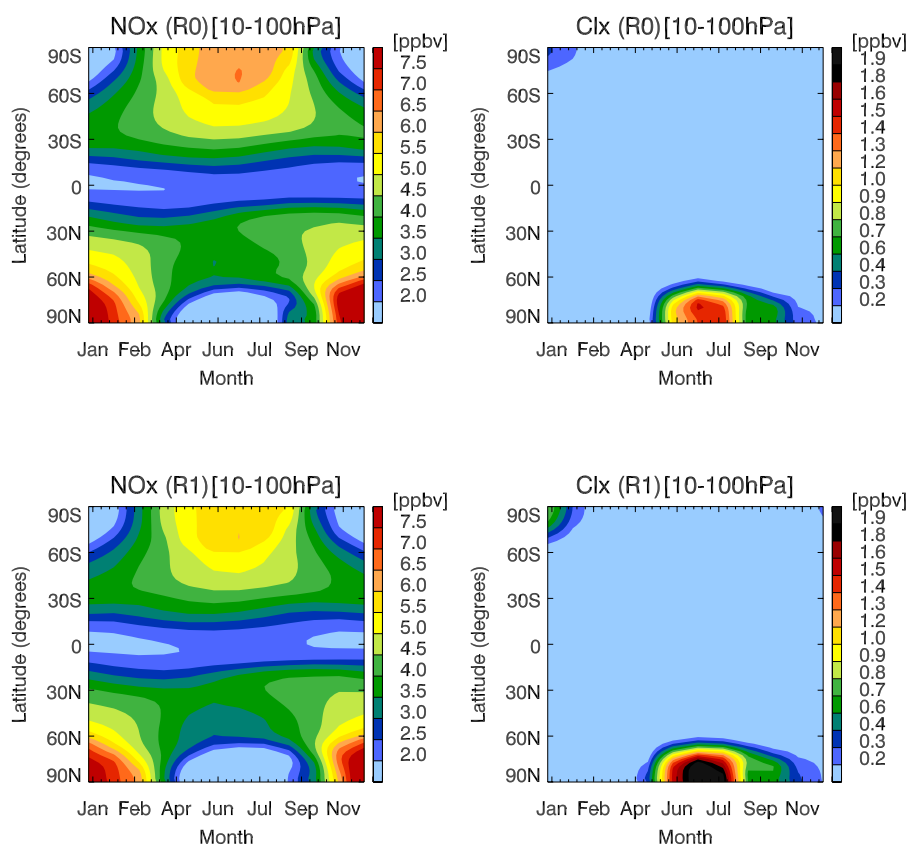


**Fig. 3.** Mean volume mixing ratios of NO<sub>x</sub> and Cl<sub>x</sub> between 10–100 hPa from R0 and R1.

in the tropics, and a maximum cooling of 4 K at high latitudes (Fig. 4). Forster and Shine (2002) found that a uniform increase of 0.7 ppmv of water vapor in the stratosphere resulted in a cooling of the polar vortices by 4–6 K in the spring and an overall cooling of the stratosphere by 0.8 K from 5 hPa to 50 hPa. Their estimated cooling is smaller than our results, possibly because their model did not include ozone-temperature feedbacks. Figure 4 indicates that column O<sub>3</sub> increases everywhere with the notable exception of the edge of the Antarctic polar vortex in the spring. The seasonal chemical O<sub>3</sub> loss is increased in the polar regions in the spring due to the stratospheric cooling (not shown). In particular, there is a prominent increase in the chemical O<sub>3</sub> loss at the edge of the Antarctic vortex, which drives the overall column decrease. The result suggests that the H<sub>2</sub>O-induced cooling has allowed the occurrence of PSCs to extend to lower latitudes.

It is worth noting that when H<sub>2</sub>O-induced cooling exceeds 4 K, the increase in the column ozone becomes smaller or even reverses, i.e., the large cooling tends to cause more ozone destruction rather than increase the column ozone. In theory, the cooling due to increased water vapor in the stratosphere raises

the threshold temperature for chlorine activation in the winter/spring polar lower stratosphere. When the temperature is near the threshold for chlorine activation, water vapor-induced cooling results in more active chlorine and more ozone loss. Elsewhere, the cooling tends to increase the column total ozone by slowing down the rate of gas-phase loss processes. The vortex-averaged ozone differences between R2 and R3 indicate that a 2-ppmv water vapor increase causes 0.2 ppmv increase in ozone in the Arctic lower stratosphere from January to February, and 0.3 ppmv in the Arctic upper stratosphere from February to March.

Note that in the Arctic stratosphere, the cooling-induced ozone changes are closely related to temperature changes. In the Antarctic stratosphere, however, the ozone changes are not well in accordance with the temperature decreases in their spatial distributions. The ozone and temperature differences shown in Fig. 5 indicate that the H<sub>2</sub>O-induced cooling is most pronounced at the SH high latitudes with a maximum cooling of about 4 K in the upper stratosphere. Elsewhere, an average cooling of 2 K can be noted. This cooling leads to a 3% O<sub>3</sub> increase in the middle and upper stratosphere and a 3% O<sub>3</sub> decrease in the tropical lower stratosphere. In the SH high latitudes lower

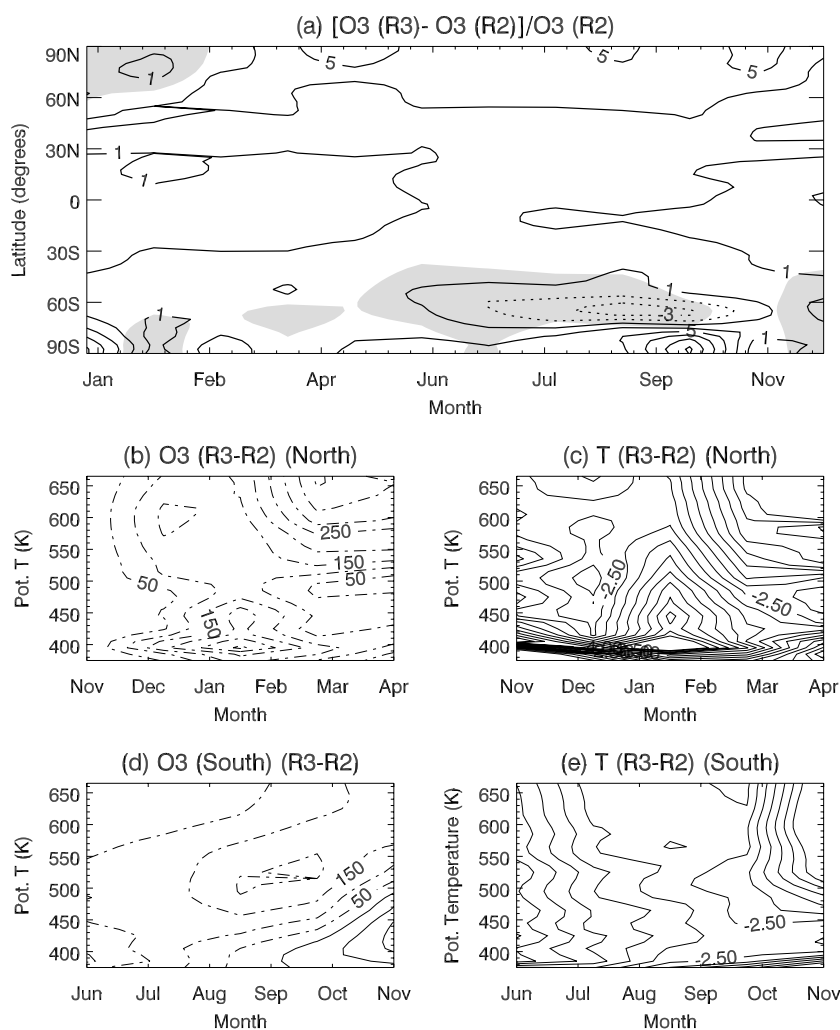


**Fig. 4.** (a) Differences (%) in the TCO between R2 and R3. The contour interval is 1% for ozone percentage changes. The regions where the stratospheric temperature in R3 (averaged between 100–10 hPa) is more than 2 K cooler than in R2 are shaded. (b)–(e) Vortex-averaged temperature and ozone differences between R2 and R3.

stratosphere, the ozone increase can reach about 4%. Evans et al. (1998) showed that increasing water vapor only causes  $O_3$  decreases in the tropical lower stratosphere, while some other modeling studies (e.g., Shindell, 2001; Dvortsov and Solomon, 2001) showed that increasing water vapor also enhances ozone depletion in the middle latitudes and polar regions. Our results indicate that the cooling effects of increasing water vapor lead to an ozone decrease in the tropics and the SH high latitudes lower stratosphere, while elsewhere ozone increases.

Figure 5 also shows the differences in chemical ozone loss,  $NO_x$ ,  $Cl_x$ , and  $Br_x$ . In the middle stratosphere, the water vapor-induced cooling depresses ozone depletion either directly through slowing of the reaction  $O+O_3 \rightarrow 2O_2$ , or indirectly by decreasing

$NO_y$  and the  $O/O_x$  ratio (Rosenfield et al., 2002). In fact, the  $NO_x$  concentrations in R3 are indeed lower than those in R2 except in the Antarctic lower stratosphere where large ozone decreases can be noted.  $Cl_x$  concentrations in R3 are much larger than those in R2 in the Arctic lower stratosphere. In the tropical lower stratosphere, both  $Cl_x$  and  $Br_x$  concentrations in R3 are lower than those in R2. Kirk-Davidoff et al. (1999) reported that ozone loss in the late winter/spring Arctic vortex critically depends on the water vapor variations, and a significant enhancement in the Arctic ozone loss can be caused by increasing water vapor. Using a simple, parameterized heterogeneous chemistry scheme, Shindell et al. (1998) showed that increasing GHGs may lead to severe ozone destruction over the Arctic. Our results show no such severe ozone

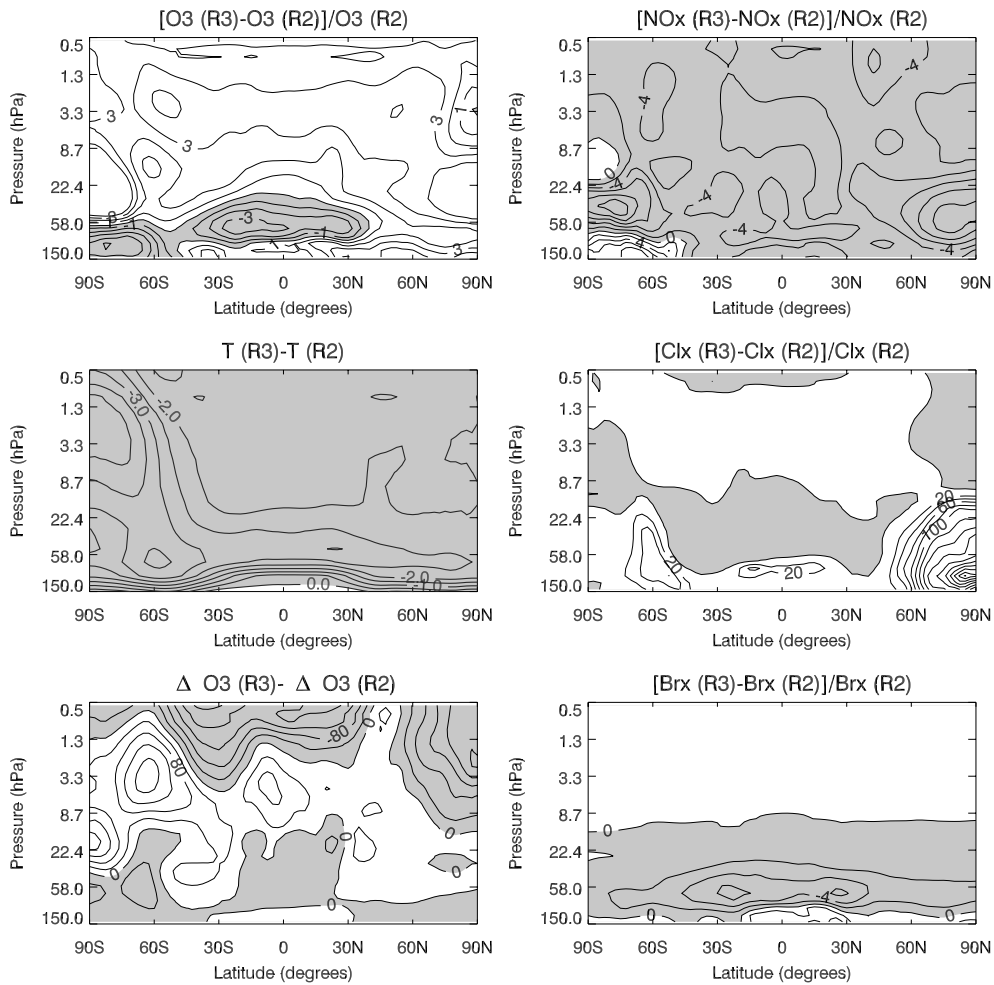


Fig. 5. Same as Fig. 2, but for the differences between R2 and R3.

depletion in the Arctic vortex due to the moderate cooling ( $\sim 2$  K) caused by an extra 2-ppmv water vapor. If the cooling is not significant enough, it may depress rather than enhance the ozone destruction within the Arctic vortex as is evident in Figs. 4 and 5. The modelling study by Oinas et al. (2001) showed that an overall cooling of the stratosphere by about 0.3 K is caused by a uniform 0.7 ppmv increase of stratospheric water vapor. This cooling is in overall agreement with our results, which is about a 1-K cooling per ppmv  $\text{H}_2\text{O}$  increase.

The seasonal variation of the differences in the ozone mixing ratios between R3 and R2 (not shown) indicates that despite the overall ozone increases caused by water vapor-induced cooling, the cooling enhances  $\text{O}_3$  loss in the Arctic upper stratosphere in January. However, pronounced decreases in ozone concentrations can be noted in the southern high latitudes upper stratosphere in July. In the tropical and Antarctic lower stratosphere, ozone loss is slightly increased throughout the year due to increased water vapor in

the model's radiation scheme.

## 5. Overall effects

We can see that increasing water vapor leads to a cooling of the stratosphere and modifies stratospheric chemical processes. The cooling of the stratosphere slows down the temperature-dependent stratospheric ozone depletion processes on one side and increases PSC formation, resulting in larger ozone losses in cold polar winters, on the other. Increasing water vapor also has a large impact on chemical processes, which destroy stratospheric  $\text{O}_3$  even without its direct cooling effects being taken into account. Figure 6 shows the vertical profiles of the global mean temperature and ozone changes between R0 and R1 and between R2 and R3. We can see that both chemical and radiative effects of increased stratospheric water vapor on ozone are pronounced, although the chemistry-related effects of increasing water vapor tend to decrease ozone, while the radiative effects lead to an increase in ozone in

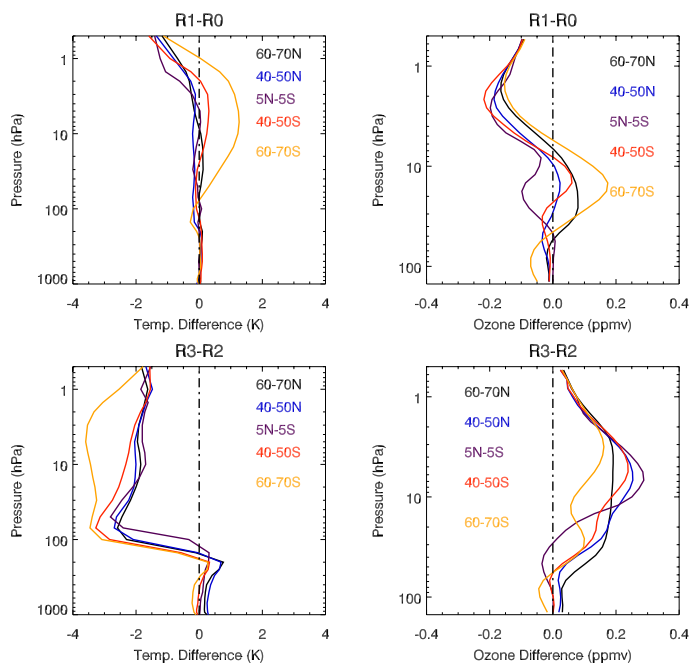


**Fig. 6.** Vertical profiles of the differences in temperature (K) and ozone (ppmv) between (top) R0 and R1 and (bottom) R2 and R3. The results are averaged over five different latitude bands.

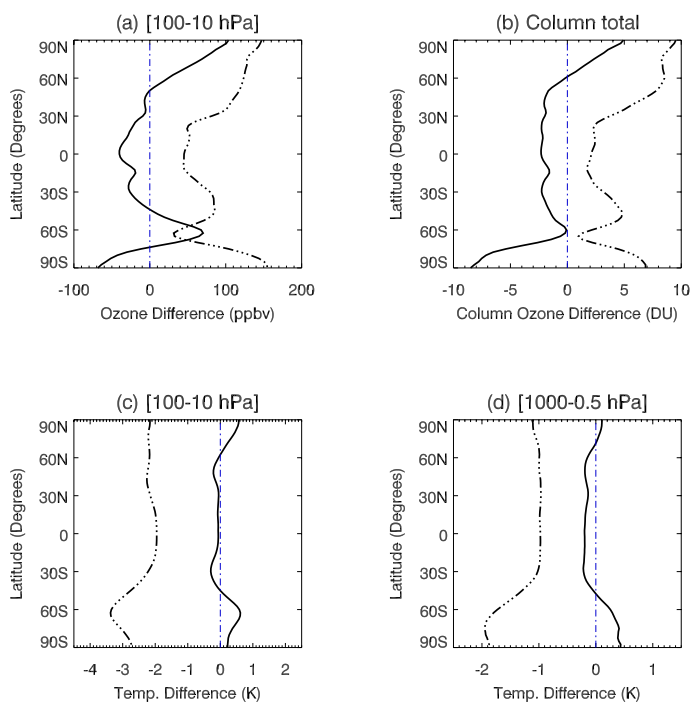


**Fig. 7.** Latitudinal distribution of the changes in (a) O<sub>3</sub> averaged between 100 hPa and 10 hPa, (b) TCO (DU), (c) temperature (K) averaged between 100 hPa and 10 hPa, and (d) temperature (K) averaged between 1000 hPa and 0.5 hPa. The solid lines represent differences between R0 and R1 and the dash-dot lines represent differences between R2 and R3.

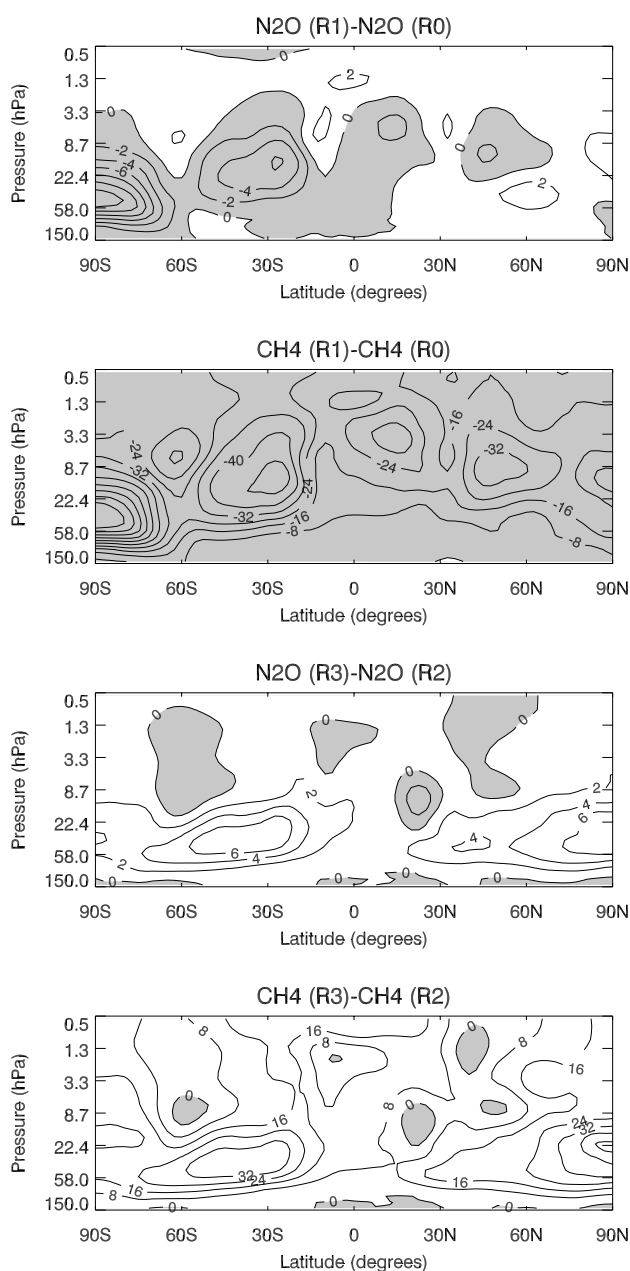


**Fig. 8.** Latitude-height cross sections of the differences in  $\text{N}_2\text{O}$  (ppbv) and  $\text{CH}_4$  (ppbv) between (top) R0 and R1 and (bottom) R2 and R3. Regions of negative changes are shaded.

the mid and upper stratosphere. The net effect of increasing water vapor tends to increase ozone in the mid stratosphere at middle and high latitudes. In the upper stratosphere, chemical and radiative effects are likely to offset each other. The temperature responses to increasing water vapor in the chemistry and radiation schemes are different. The radiative cooling of increasing water vapor is much larger over all latitudes, ranging from 1 K to 4 K. The chemical effect of increasing water vapor gives rise to a cooling only in the

upper stratosphere, while in the Antarctic middle and upper stratosphere, a warming of about 1 K can be noted. The chemical and radiative effects of increased water vapor together lead to less cooling at the southern high latitudes than they do separately.

Figure 7 shows the latitude distributions of the temperature and ozone changes between R0 and R1 and between R2 and R3. The ozone mixing ratios (averaged between 100 hPa and 10 hPa) have decreased by  $\sim 20$  ppbv over the  $50^\circ\text{S}$  to  $50^\circ\text{N}$  latitude range due to a 2-ppmv water vapor increase in the model's chemistry scheme and have increased by  $\sim 40$  ppbv due to a 2-ppmv increase in the model's radiation scheme (Fig. 7). The net effect of the increasing water vapor may thus slightly increase the ozone mixing ratios over the  $50^\circ\text{S}$  to  $50^\circ\text{N}$  latitude range. In the Antarctic stratosphere, the chemical effects decrease the ozone, while the radiative effects increase the ozone, so these processes offset each other. In the Arctic stratosphere, however, both the chemical and radiative effects tend to increase ozone.

For the TCO, again, both the radiative and chemical related effects of increasing water vapor give rise to increased TCO values at the northern high latitudes, while at the southern high latitudes the chemical effect tends to decrease the TCO, but the radiative effect is likely to increase the TCO. Increasing stratospheric water vapor cools the stratosphere both directly through radiative effects and indirectly through its chemical effects, except at the polar regions where there is a slight warming due to the chemical effects. The combined effect of the increased stratospheric water vapor will give rise to more significant cooling in the tropics and the middle latitudes, but less cooling in the polar stratosphere. On a global average, a 2-ppmv  $\text{H}_2\text{O}$  increase in the chemistry scheme will lead to a decrease of the TCO by 1.6 DU (not shown). However, a 2-ppmv  $\text{H}_2\text{O}$  increase in the radiation scheme leads to an increase of the TCO by 4.7 DU. It is apparent that the radiative effects of increasing water vapor on the TCO are more significant than the chemical effects. Tabazadeh et al. (2000) also showed that the radiative effect of water vapor is larger than its effects on chemistry and microphysics. An overall increase of the TCO and decrease of the stratospheric temperature can be expected if stratospheric water vapor increases by 2 ppmv. However, the combined chemical and radiative effects of increasing water vapor may not be as significant due to offsetting effects.

For long-lived chemical species like  $\text{CH}_4$  and  $\text{N}_2\text{O}$ , changes in their distribution mainly reflect changes in transport processes. Figure 8 shows the latitude-height cross sections of the differences in  $\text{N}_2\text{O}$  and  $\text{CH}_4$  between runs R0 and R1, and R2 and R3. It is appar-

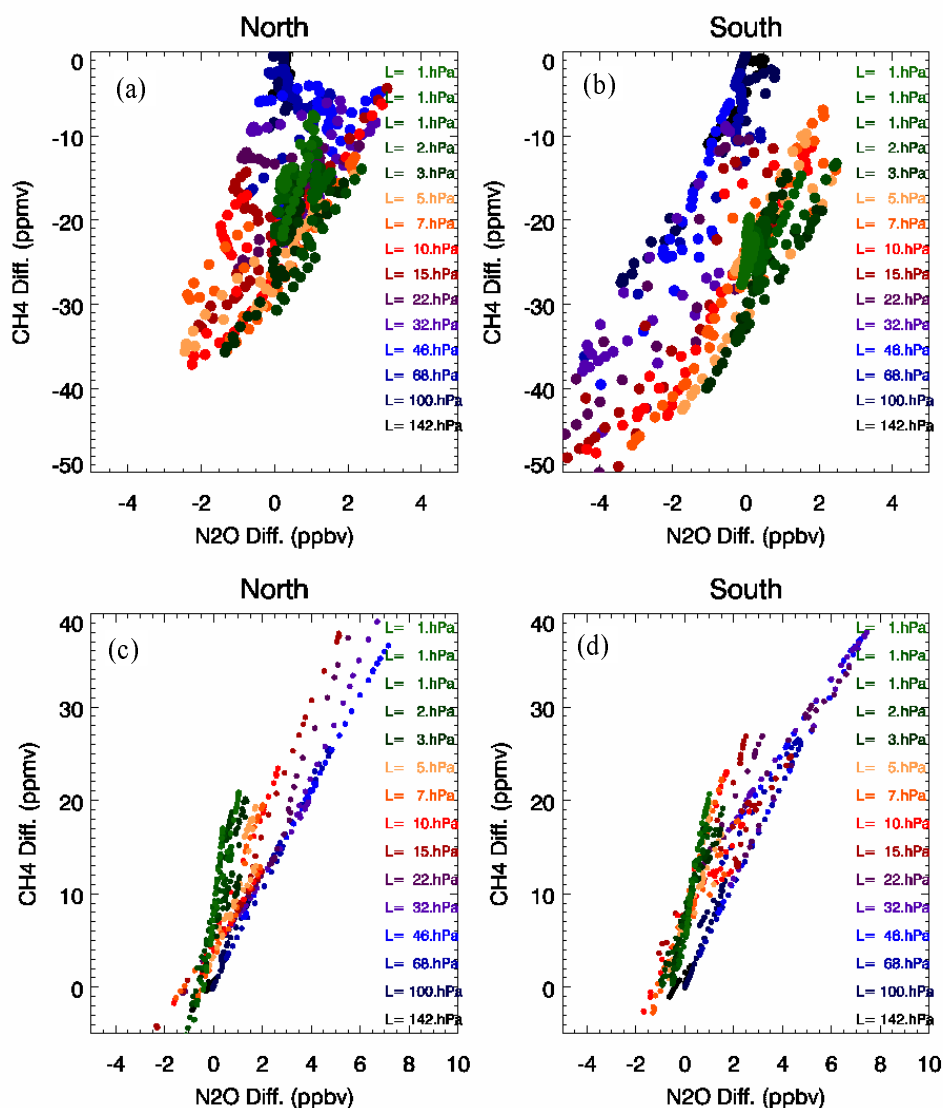


**Fig. 9.** Correlation plots of the differences in  $\text{CH}_4$  and  $\text{N}_2\text{O}$  (ppbv) between (a, b) R0 and R1 and (c, d) R2 and R3. Each circle represents a model latitude-height grid point at which differences in zonal mean climatology of  $\text{CH}_4$  and  $\text{N}_2\text{O}$  between two experiments are calculated. The data are shown for both hemispheres and the colors indicate the model levels.

ent that  $\text{CH}_4$  concentrations in R1 are overall smaller than those in R0. The time series of  $\text{CH}_4$  mixing ratios on the 10 hPa level indicate that  $\text{CH}_4$  concentrations in R1 are lower than those in R0 throughout the integrations (not shown). Note that the differences in  $\text{CH}_4$  between R0 and R1 are also related to the enhanced oxidation caused by the increased OH from the increased  $\text{H}_2\text{O}$ . Therefore, the information on transport changes between R0 and R1 cannot be inferred directly from  $\text{CH}_4$  differences shown in Fig. 8. However, the average  $\text{CH}_4$  between 10–100 hPa from R0 and R1 in-

dicates that the descent in the Arctic spring is stronger in R1 than in R0 (not shown), and this is consistent with increases in the TCO in the Arctic spring despite the increased chemical ozone loss. The changes in  $\text{N}_2\text{O}$  show a similar pattern to  $\text{CH}_4$ . A decrease of  $\text{N}_2\text{O}$  can be noted in the SH middle and lower stratosphere. However, in the NH stratosphere, the  $\text{N}_2\text{O}$  concentrations in R1 are slightly larger than those in R0, and therefore do not show such a clear signal of an enhanced descent in the annual mean. The differences in the  $\text{N}_2\text{O}$  and  $\text{CH}_4$  fields between R2 and R3 show

that  $\text{CH}_4$  concentrations in R3 are overall higher than those in R2, implying that water vapor-induced cooling enhances the transport of  $\text{CH}_4$  from the troposphere to the stratosphere. Recall that an increase of 2-ppmv  $\text{H}_2\text{O}$  in the chemistry scheme leads to a decrease in  $\text{CH}_4$  and  $\text{N}_2\text{O}$  concentrations. We can also see that the  $\text{N}_2\text{O}$  and  $\text{CH}_4$  differences between R0 and R1 are about twice as large as those between R2 and R3 owing to more significant chemical contributions in R0 and R1.

Figure 9 further shows the correlation plots of the  $\text{CH}_4$  and  $\text{N}_2\text{O}$  differences between runs R0 and R1. Since both  $\text{CH}_4$  and  $\text{N}_2\text{O}$  are long-lived chemical species, their changes will be proportional to each other if the changes are mainly caused by dynamical processes. We can note that the  $\text{CH}_4$  and  $\text{N}_2\text{O}$  changes have a broadly linear correlation, particularly in the SH. In the NH lower stratosphere, the correlations are less significant. The results here suggest that  $\text{CH}_4$  changes are both dynamically and chemically controlled, while the dynamical responses to increasing water vapor in the NH are more pronounced than in the SH. The correlations between the  $\text{CH}_4$  and  $\text{N}_2\text{O}$  differences between runs R2 and R3 show that the  $\text{CH}_4$  and  $\text{N}_2\text{O}$  changes have a fairly good linear correlation. The correlations are significant in both hemispheres and more compact than those for R0 and R1. Figure 9 confirms that increased water vapor in the chemistry scheme has both chemical and dynamical impacts on  $\text{CH}_4$  concentrations, while  $\text{N}_2\text{O}$  changes are predominately controlled by the dynamical processes.

## 6. Effect of increasing water vapor on ozone recovery

The 3D CCM simulations of the ozone layer from 1979–2055 by Austin et al. (2000, 2001) showed that an increase in GHGs tends to delay the onset of ozone recovery, and ozone had still not returned to 1980 conditions by 2054. In their simulations, only the ozone field was coupled to the GCM radiation scheme. Using a fully coupled CCM in which  $\text{O}_3$ ,  $\text{CH}_4$  and  $\text{N}_2\text{O}$  from the chemistry module were coupled to the model's radiation scheme, Tian and Chipperfield (2004) predicted that column  $\text{O}_3$  would be about 5% higher in 2050 than present day values in the tropics, about 15% higher in the Arctic winter/spring, and up to 90% higher in the Antarctic  $\text{O}_3$  hole. It is interesting to know whether the coupling of water vapor will make a difference in the prediction of the ozone layer by 2050 and 2100 and whether increasing water vapor could delay the ozone recovery. Figure 10 shows the 10-year averaged TOMS data (for the period 1993–2000) and the modeled monthly mean TCO for March in the NH and for October in the SH in 2000. Also shown are the differences in the TCO for corresponding months between 2050 and 2000 and between 2100 and 2000. A comparison of the modeled TCO climatology for the 2000 conditions with the corresponding TOMS observations for the period 1993–2000 indicates that both the magnitudes and the geographical distribution of the monthly mean TCO in the NH and the SH are reasonably simulated by the CCM. It should be pointed

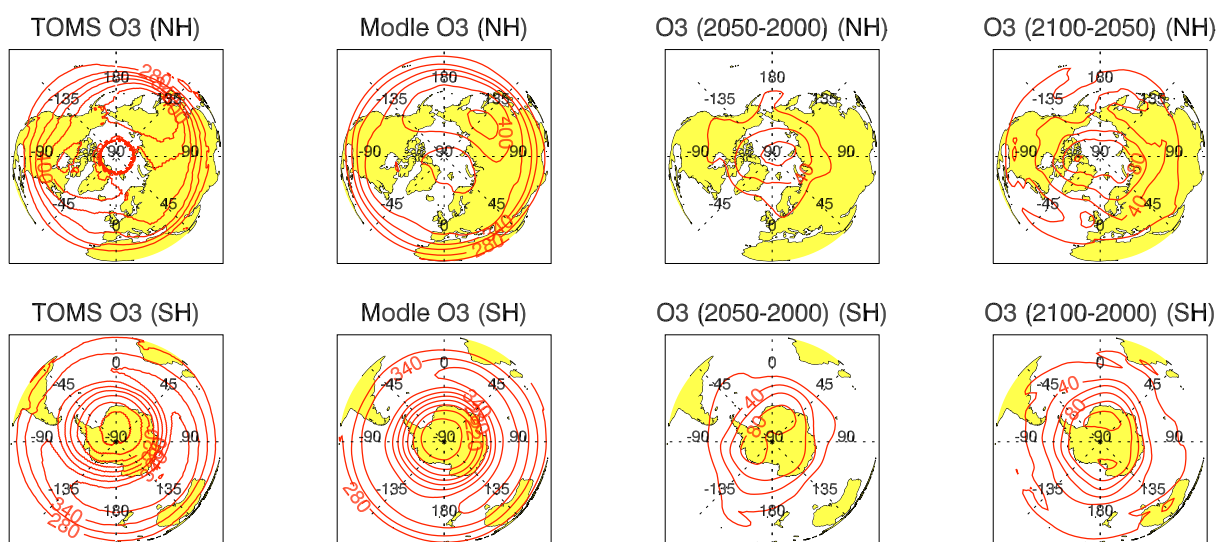


**Fig. 10.** The 10-year averaged model and TOMS monthly mean TCO (DU) for the NH March and the SH October for 2000. Also shown are the differences in the total ozone for corresponding months between 2050 and 2000, and between 2100 and 2000. The contour interval is 30 DU for the TCO, and 20 DU for the differences. Yellow area represents topography.

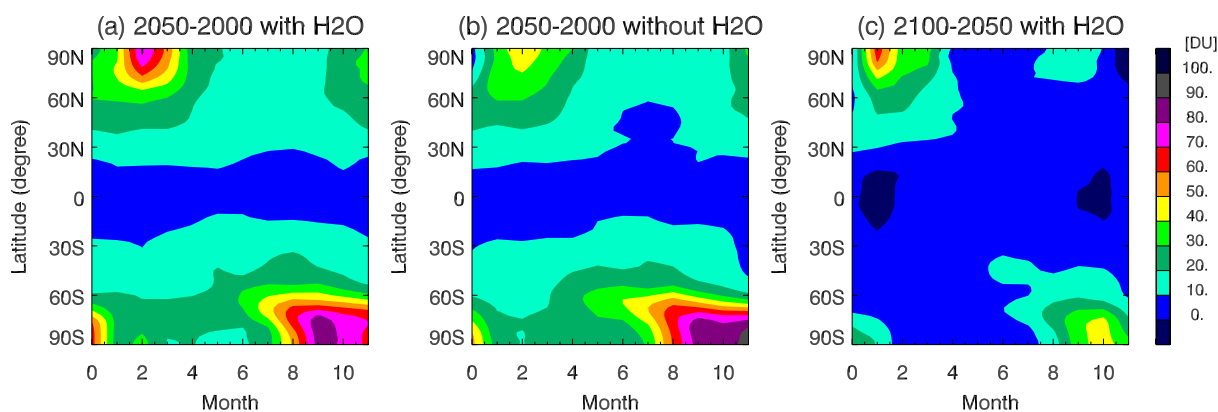


**Fig. 11.** Seasonal variations of the zonal mean TCO differences (DU) (a) between R4 and R2, and (c) between R5 and R4. The corresponding difference between the 2000 and 2050 runs described in Tian and Chipperfield (2004), in which the water vapor was not coupled to the radiation scheme, is also shown for comparison (b).

**Table 3.** The 10-year averaged global mean temperature ( $T_g$ ), column ozone, stratospheric temperature ( $T_s$ ) and age-of-air averaged between 100 to 0.5 hPa for the 2000, 2050, and 2100 predictions.

Year	O <sub>3</sub> (DU)	$T_g$ (K)	$T_s$ (150–0.5 hPa) (K)	Age of air (yr)
2000	251	238.8	230.8	3.257
2050	271	236.3	227.7	3.267
2100	279	233.5	223.3	3.189

out that a tropospheric column ozone climatology from Logan (1999) has been added to the model climatology in Fig. 10 as the modelled ozone column only covers 150–0.5 hPa. Relative to the modelled TCO for 2000, we can see a significant ozone recovery in both hemispheres for the 2050 and 2100 TCO values. By 2100, a 100-DU TCO increase is reached in the Arctic while a 120-DU increase can be noted in the Antarctic. Also noticeable is that the recovery for the period from 2000 to 2050 is much more significant than that from 2050 to 2100, which reflects the larger relative change in chlorine loading in the earlier period (Table 2).

Figure 11 shows variations of the zonal mean TCO differences between R4 and R2 and between R5 and R4. Also shown are the corresponding differences between the 2000 and 2050 runs described in Tian and Chipperfield (2004) in which the chemistry water vapor was not coupled to the radiation scheme but the UM specific humidity field was used in the radiation scheme. Note that the coupling of the chemistry water vapor to the radiation scheme gives rise to more ozone recovery in the northern high latitude spring but slightly less ozone recovery in the southern high latitudes in winter. The results here are in agreement with our integrated perspective in Section 6 since the UM water vapor is much smaller than the chemistry water vapor, i.e., increasing water vapor tends to accelerate the ozone recovery in the Arctic but slightly

delay recovery in the Antarctic. Consistent with Fig. 10, the ozone recovery from 2000 to 2050 is more significant than that from 2050 to 2100.

Table 3 lists the 10-year averaged global mean temperature, the column ozone, the stratospheric temperature and the age-of-air averaged between 100 to 0.5 hPa for the 2000, 2050, and the 2100 predictions. It is evident that ozone recovery is not simply proportional to the cooling; changes in halogen loading are clearly a dominant factor. From 2000 and 2050, a 20-DU recovery corresponds to a 2.5-K cooling of the global mean temperature and a 3.1 K cooling in the stratosphere. From 2050 to 2100, however, an 8-DU ozone recovery corresponds to a 2.8-K cooling of the global mean temperature and a 4.4-K cooling in the stratosphere. The change in the age-of-air in the stratosphere is not pronounced although the air becomes younger from 2000 to 2100.

## 7. Summary and conclusions

Increasing water vapor can change stratospheric ozone through radiative effects and through heterogeneous or HO<sub>x</sub>-related gas-phase chemistry. This wide range of effects, and the feedbacks between them, means that a good, quantitative assessment of its potential impact on future ozone and climate is a very complex task. Using a detailed and interactively coupled CCM, we have investigated the chemical and

radiative effects of stratospheric water vapor on the ozone layer and temperature separately through a prescribed increase of H<sub>2</sub>O in the model's chemistry and radiation scheme.

The chemistry-induced effects of increasing water vapor lead to an overall decrease of the TCO by about 1% in the tropics and by a maximum of 12% at southern high latitudes. At northern high latitudes, the TCO is increased by no more than 5% due to chemical effects of a 2-ppmv additional water vapor. Radiative effects of a 2-ppmv H<sub>2</sub>O increase cause a 2-K cooling in the tropical stratosphere and more than a 4-K cooling at high latitudes. This cooling leads to an increase of the TCO by about 2%–6%. However, when the cooling exceeds about 5 K, the TCO values at high latitudes decrease rather than increase. The ozone changes and temperature changes associated with increasing stratospheric water vapor lead to dynamical responses of the atmosphere. A 2-ppmv H<sub>2</sub>O increase in the chemistry scheme leads to stronger descent in the Arctic spring. The dynamic responses induced by increasing stratospheric water have an evident inter-hemisphere asymmetry.

A 2-ppmv H<sub>2</sub>O increase in the chemistry gives rise to a decrease of the global mean TCO by 1.5 DU. However, the radiative effects of a 2-ppmv H<sub>2</sub>O increase of water vapor leads to an increase of the TCO by 4.8 DU. Correspondingly, the global mean temperature is decreased by 2.8 K due to radiative effects of a 2-ppmv H<sub>2</sub>O increase, while the chemical effects of a 2-ppmv H<sub>2</sub>O increase have a small impact on the global mean temperature.

Although the direct cooling effect of increasing water vapor is partly offset by its chemical effect in the southern high latitudes, in the northern high latitudes, both the chemical and radiative effects tend to increase ozone. It is apparent that the combined effects of increasing water vapor on the ozone layer and temperature, and the corresponding feedbacks between dynamic and chemical processes, are important factors influencing future climate and ozone recovery. Increasing stratospheric water vapor tends to accelerate ozone recovery in the northern high latitudes and slightly delay the recovery in the southern high latitudes. CCM studies of the future recovery of the ozone layer should pay attention to water vapor trends predicted or imposed in the model runs.

Our CCM experiments all used the same fixed SSTs. However, the GHG-induced global warming will change SSTs, while SST changes in turn have a profound impact on temperature and circulation as well as the water vapor concentrations in both the stratosphere and troposphere. A more complete understanding of the impact of water vapor changes on ozone de-

pletion and climate change requires a whole chemistry-climate model in which various feedbacks between water vapor, ozone, temperature, SSTs and circulation changes should be included.

**Acknowledgements.** This research was supported by National Natural Science Foundation of China (Grant Nos. 40575019, 40730949) and the U.K. Natural Environment Research Council (NERC). We thank NCAS for computational support. We also thank two anonymous reviewers for their helpful comments.

## REFERENCES

- Austin, J., N. Butchart, and K. P. Shine, 1992: Possibility of an Arctic ozone hole in a doubled-CO<sub>2</sub> climate. *Nature*, **360**, 221–225.
- Austin, J., N. Butchart, and J. Knight, 2000: Three-dimensional chemical model simulations of the ozone layer: 1979–2015. *Quart. J. Roy. Meteor. Soc.*, **126**, 1533–1556.
- Austin, J., N. Butchart, and J. Knight, 2001: Three-dimensional chemical model simulations of the ozone layer: 2015–2055. *Quart. J. Roy. Meteor. Soc.*, **127**, 959–974.
- Chipperfield, M. P., 1999: Multiannual simulation with a three-dimensional chemical transport model. *J. Geophys. Res.*, **104**, 1781–1805.
- Cullen, M. J. P., 1993: The unified forecast/climate model. *Meteor. Mag.*, **122**, 81–94.
- Dameris, M., V. Grewe, R. Hein, C. Schnadt, C. Bruhl, and B. Steil, 2001: Assessment of the future development of the ozone layer. *Geophys. Res. Lett.*, **25**, 3579–3582.
- Dvortsov, V., and S., Solomon, 2001: Response of the stratospheric temperatures and ozone to past and future increases in stratospheric humidity. *J. Geophys. Res.*, **106**, 7505–7514.
- Evans, S. J., R. Toumi, J. E. Harries, M. P. Chipperfield, and J. M. Russel III, 1998: Trends in stratospheric humidity and the sensitivity of ozone to these trends. *J. Geophys. Res.*, **103**, 8715–8725.
- Forster, P. M. de F., and K. P. Shine, 1999: Stratospheric water vapor changes as a possible contributor to observed stratospheric cooling. *Geophys. Res. Lett.*, **26**, 3309–3312.
- Forster, P. M. de F., and K. P. Shine, 2002: Assessing the climate impact of trend in stratospheric water vapor. *Geophys. Res. Lett.*, **29**, doi: 10.1029/2001GL013909.
- Kirk-Davidoff, D. B., E. J. Hints, J. G. Anderson, and D. W. Keith, 1999: The effect of climate change of ozone depletion through changes in stratospheric water vapour. *Nature*, **402**, 399–401.
- Logan, J. A., 1999: An analysis of ozone sonde data for the troposphere recommendations for testing 3-D models, and development of a gridded climatology for tropospheric ozone. *J. Geophys. Res.*, **104**,

- 16115–16149.
- Nedoluha, G. E., and Coauthors, 1998: Increases in middle atmospheric water vapor as observed by HALOE and the ground based Water Vapor Millimeter-wave Spectrometer from 1991–1997. *J. Geophys. Res.*, **103**, 3531–3543.
- Oinas, V., A. A., Lasis, D., Rind, D. T., Shindell, and J. E., Hansen, 2001: Radiative cooling by stratospheric water vapor: Big difference in GCM results. *Geophys. Res. Lett.*, **28**, 2791–2794.
- Oltmans, S. J., H. Vomel, D. J. Hofmann, K. H. Rosenlof, and D. Kley, 2000: The increase in stratospheric water vapor from balloon-borne, frostpoint hygrometer measurements at Washington, D. C., and Boulder, Colorado. *Geophys. Res. Lett.*, **27**, 3453–3456.
- Pitari, G., S. Palmeri, G. Visconti, and R. G. Prinn, 1992: Ozone response to a CO<sub>2</sub> doubling: Results from a stratospheric circulation model with heterogeneous chemistry. *J. Geophys. Res.*, **97**, 5953–5962.
- Rind, D., and P. Logergan, 1995: Modelled impacts of stratospheric ozone and water vapor perturbations with implications for high-speed civil transport aircraft. *J. Geophys. Res.*, **100**, 7381–7396.
- Rosenfield, J. E., A. R. Douglass, and D. B. Considine, 2002: The impact of increased carbon dioxide on ozone recovery. *J. Geophys. Res.*, **107**(D6), doi: 10.1029/2001JD000824.
- Shine, K. P., and Coauthors, 2003: A comparison of model-simulated trends in stratospheric temperature. *Quart. J. Roy. Meteor. Soc.*, **129**, doi: 10.1256/qj.02.186.
- Shindell, D. T., 2001: Climate and ozone response to increased stratospheric water vapor. *Geophys. Res. Lett.*, **28**, 1551–1554.
- Shindell, D. T., and V. Grewe, 2002: Separating the influence of halogen and climate changes on ozone recovery in the upper stratosphere. *J. Geophys. Res.*, **107**(D12), doi: 10.1029/2001JD000420.
- Shindell, D. T., D. Rind, and P. Lonergan, 1998: Increased polar stratospheric ozone losses and delayed eventual recovery owing to increasing greenhouse-gas concentrations. *Nature*, **392**, 589–592.
- Smith, C. A., J. D. Haigh, and R. Toumi, 2001: Radiative forcing due to trends in stratospheric water vapor. *Geophys. Res. Lett.*, **28**, 179–182.
- Stuber, N., M. Ponater, and R. Sausen, 2001: Is the climate sensitivity to ozone perturbations enhanced by stratospheric water vapor feedback. *Geophys. Res. Lett.*, **28**, 2887–2890.
- Stenke, A., and V. Grewe, 2005: Simulation of stratospheric water vapor trends: Impact on stratospheric ozone chemistry. *Atmospheric Chemistry and Physics*, **5**, 1257–1272.
- Tabazadeh, A., M. L. Santee, M. Y. Danlin, H. C. Pumphrey, P. A. Newman, P. J. Hamill, and J. L. Mergenthaler, 2000: Quantifying denitrification and its effect on ozone recovery. *Science*, **288**, 1407–1411.
- Tian, W. S., and M. P. Chipperfield, 2004: A new coupled chemistry-climate model for the stratosphere: The importance of coupling for future O<sub>3</sub>-climate predictions. *Quart. J. Roy. Meteor. Soc.*, **131**, 281–303, doi: 10.1256/qj.04.05.
- Tian, W. S., and M. P. Chipperfield, 2006: Stratospheric water vapor trends in a coupled chemistry-climate model. *Geophys. Res. Lett.*, **33**, L06819, doi: 10.1029/2005GL024675.
- World Meteorological Organization, 2003: *Scientific Assessment of Ozone Depletion: 2002*. WMO Global Ozone Research and Monitoring Project-Report No. 47, Geneva, Switzerland, 498pp.